Toxicology and Applied Pharmacology 291 (2016) 46–57

Contents lists available at ScienceDirect

Toxicology and Applied Pharmacology

journal homepage: www.elsevier.com/locate/ytaap

Small structural changes on a hydroquinone scaffold determine the complex I inhibition or uncoupling of tumoral oxidative phosphorylation

Félix A. Urra [a,*], Miguel Córdova-Delgado [b], Michel Lapier [a], Andrea Orellana-Manzano [a], Luis Acevedo-Arévalo [b], Hernán Pessoa-Mahana [b], Jaime M. González-Vivanco [b], Maximiliano Martínez-Cifuentes [c], Oney Ramírez-Rodríguez [b], Juan Pablo Millas-Vargas [b], Boris Weiss-López [d], Mario Pavani [a], Jorge Ferreira [a,*], Ramiro Araya-Maturana [c,*]

[a] Programa de Farmacología Molecular y Clínica, Instituto de Ciencias Biomédicas (ICBM), Facultad de Medicina, Universidad de Chile, Independencia 1027, Casilla 7, Santiago, Chile
[b] Departamento de Química Orgánica y Físico-Química, Facultad de Ciencias Químicas y Farmacéuticas, Universidad de Chile, Casilla 233, Santiago 1, Chile
[c] Instituto de Química de Recursos Naturales, Universidad de Talca, Casilla 747, Talca, Chile
[d] Departamento de Química, Facultad de Ciencias, Universidad de Chile, Casilla 653, Santiago, Chile

ARTICLE INFO

Article history:
Received 22 September 2015
Revised 12 December 2015
Accepted 15 December 2015
Available online 19 December 2015

Keywords:
Anti-cancer agents
Hydroquinones
Uncouplers
Oxidative phosphorylation
Complex I

ABSTRACT

Mitochondria participate in several distinctiveness of cancer cell, being a promising target for the design of anti-cancer compounds. Previously, we described that *ortho*-carbonyl hydroquinone scaffold **14** inhibits the complex I-dependent respiration with selective anti-proliferative effect on mouse mammary adenocarcinoma TA3/Ha cancer cells; however, the structural requirements of this hydroquinone scaffold to affect the oxidative phosphorylation (OXPHOS) of cancer cells have not been studied in detail. Here, we characterize the mitochondrial metabolism of TA3/Ha cancer cells, which exhibit a high oxidative metabolism, and evaluate the effect of small structural changes of the hydroquinone scaffold **14** on the respiration of this cell line. Our results indicate that these structural changes modify the effect on OXPHOS, obtaining compounds with three alternative actions: inhibitors of complex I-dependent respiration, uncoupler of OXPHOS and compounds with both actions. To confirm this, the effect of a bicyclic hydroquinone (**9**) was evaluated in isolated mitochondria. Hydroquinone **9** increased mitochondrial respiration in state 4o without effects on the ADP-stimulated respiration (state 3_{ADP}), decreasing the complexes I and II-dependent respiratory control ratio. The effect on mitochondrial respiration was reversed by 6-ketocholestanol addition, indicating that this hydroquinone is a protonophoric uncoupling agent. In intact TA3/Ha cells, hydroquinone **9** caused mitochondrial depolarization, decreasing intracellular ATP and NAD(P)H levels and GSH/GSSG ratio, and slightly increasing the ROS levels. Moreover, it exhibited selective NAD(P)H availability-dependent anti-proliferative effect on cancer cells. Therefore, our results indicate that the *ortho*-carbonyl hydroquinone scaffold offers the possibility to design compounds with specific actions on OXPHOS of cancer cells.

1. Introduction

Cancer cells exhibit different metabolic organization compared to normal cells (Jose et al., 2011), existing several predominant metabolic phenotypes, depending on the type of cancer (Obre and Rossignol, 2015). It has long been described the high glycolysis rate in aerobic conditions (Warburg effect) with reduced or damaged mitochondrial function in some cancer cells (Cuezva et al., 2002; Wu et al., 2007; Bellance et al., 2009); however, a large amount of evidence have demonstrated the existence of cancer cells with a high oxidative phenotype, having a functional mitochondria (Moreno-Sánchez et al., 2014). This phenotype is observed in some lymphomas (Jitschin et al., 2014), melanomas (Barbi de Moura et al., 2012), and breast cancer (Diers et al., 2013), showing dependence on oxidative phosphorylation (OXPHOS) for the supply of ATP and availability of intermediates of tricarboxylic acid (TCA) cycle, required for survival and growth (Zu and Guppy, 2004; Moreno-Sánchez et al., 2014).

Mitochondrial respiration occurs in the electron transport chain (ETC), which is composed by the respiratory complexes I, II, III and IV. The ETC activity depends on the availability of NADH and $FADH_2$ from TCA cycle, which are oxidized by complexes I and II, being molecular

Abbreviations: ROS, reactive oxygen species; OXPHOS, oxidative phosphorylation; ANT, adenine nucleotide translocator; CCCP, carbonyl cyanide m-chlorophenylhydrazone; RCR, respiratory control ratio; ETC, electon transport chain; $\Delta\Psi m$, mitochondrial membrane potential; OCR, oxygen consumption rate; NAC, N-acetyl L-cysteine; RRI, relative resistance index; mPTP, mitochondrial permeability transition pore; TMPD, N,N,N′,N′-tetramethyl-*p*-phenylenediamine.

* Corresponding authors.
E-mail addresses: felix.urra@qf.uchile.cl (F.A. Urra), jferreir@med.uchile.cl (J. Ferreira), raraya@utalca.cl (R. Araya-Maturana).

http://dx.doi.org/10.1016/j.taap.2015.12.005
0041-008X/

oxygen the final acceptor (Brand and Nicholls, 2011). The energy released in the transfer of electrons is used to pump protons from the matrix into the intermembrane space by complexes I, III and IV, generating a proton-based electrochemical gradient. Dissipation of this gradient through FoF_1-ATP synthase drives ADP phosphorylation (Mitchell, 1961). Complex I has an important control in the electron transfer (Rodríguez-Enríquez et al., 2000) and contributes about 40% of the proton motive force required for mitochondrial ATP synthesis (Galkin et al., 2006; Zickermann et al., 2015). The coupling between these redox reactions and ATP synthesis varies among cell lines and in pathophysiological conditions, such as cancer, leading to different pattern of energetic metabolisms (Jose et al., 2011). The modification of this coupling through the modulation of mitochondrial respiration has emerged as a potential therapeutic target to obtain new anti-cancer compounds, especially in cancer cells with a high oxidative phenotype. Interestingly, several compounds with anti-cancer actions selectively modulate the mitochondrial respiration by inhibiting of the electron flow at complex I level (Hail and Lotan, 2004; Pereira et al., 2007; Chen et al., 2011; de Pedro et al., 2013) or by uncoupling of OXPHOS (Han et al., 2009; Pardo-Andreu et al., 2011), producing a decreased proliferation and cell death.

Previously, we have described that antioxidant *para*-hydroquinones, which incorporate a carbonyl group in the *ortho*-position to one of the phenolic hydroxyl groups, inhibit the respiration of cancer cells (Araya-Maturana et al., 2002, 2006; Rodríguez et al., 2007). One of them, the hydroquinone **14**, 9,10-dihydroxy-4,4-dimethyl-5,8-dihydroanthracen-1(4*H*)-one (Fig. 2A), affects selectively the proliferation of mammary cancer cells, inducing cell cycle arrest in the G2/M phase (Urra et al., 2013). This effect is consequence of a dysfunction in the mitochondrial bioenergetics by the electron flow inhibition through complex I, leading to ADP-stimulated oxygen consumption inhibition, transmembrane potential dissipation, and cellular ATP level decrease (Urra et al., 2013). Despite this proposed mechanism, the structural requirements of this hydroquinone scaffold to affect the OXPHOS of cancer cells have not been studied in detail. On the basis of these considerations, we explore the effect of structural modifications on *ortho* carbonyl hydroquinone scaffold, structurally related to hydroquinone **14**, on the coupled and uncoupled respiration using mouse mammary adenocarcinoma TA3/Ha cells, which exhibits a high oxidative metabolism as here we describe. Our results indicate that the effect of *ortho* carbonyl hydroquinone on OXPHOS is modified with structural changes, allowing obtaining compounds with three alternative types of actions: inhibitors of complex I dependent-respiration, uncouplers of OXPHOS and compounds with both actions (dual agents). Besides, the effect of a bicyclic hydroquinone (**9**) that affected the OXPHOS with selective anti-proliferative effects on TA3/Ha cancer cells is described.

2. Materials and methods

2.1. Compounds and reagents

All reagents were obtained from Sigma-Aldrich Corp. (St. Louis, MO, USA). Stock solutions of all hydroquinones were prepared in dimethyl sulfoxide (DMSO).

2.2. Chemicals

Duroquinol was synthesized by reduction from duroquinone as previously described (Plaza et al., 2008). ^1H and ^{13}C NMR spectra were obtained from a Bruker AVANCE DRX 300 spectrometer operating at either 300.13 MHz (^1H) or 75.47 MHz (^{13}C). Measurements were carried out at 300 K in $CDCl_3$. Chemical shifts are reported as ppm downfield from TMS for ^1H NMR and relative to the central $CDCl_3$ resonance (77.0 ppm) for ^{13}C NMR. All melting points are uncorrected and were determined on a Kofler hot stage apparatus. IR spectra (KBr discs) were recorded on an FT-IR Bruker IFS 55 spectrophotometer; wave numbers are reported in cm^{-1}. High resolution mass spectra were obtained on a MAT 95XP Thermo Finnigan spectrometer. Hydroquinones **8**, **9**, **11** and **14**–**21** were synthesized by published procedures (Araya-Maturana et al., 1999, 2006, 2002; Mendoza et al., 2005; Vega et al., 2009; Dobado et al., 2011). The new compounds were synthesized as described in the Supplementary Fig. 1 and in "Synthesis and Spectra Analysis" section.

2.3. Cell lines

Mouse mammary adenocarcinoma TA3/Ha cell line was kindly provided by Dr. Gabriel Jose Gasic, University of Pennsylvania, and has been used by our laboratory since 1989 (Fones et al., 1989). TA3-MTXR methotrexate-resistant cell line was generated as described previously by us (Araya-Maturana et al., 2002; Urra et al., 2013). This cell line exhibits methotrexate resistance and cross-resistance to cisplatin, doxorubicin, 5-fluorouracil and vinblastine (Plaza et al., 2008). Mouse mammary epithelial MM3MG and NMuMG cell lines, human acute lymphoblastic leukemia CCRF-CEM cell line, and its camptothecin resistant variant, CEM/C2 were purchased from American Tissue Culture Collection (ATCC). All cells were grown in DMEM high-glucose (MM3MG, TA3/Ha and TA3-MTXR), RPMI-1640 (CCRF-CEM and CEM/C2) or RPMI-1640 plus insulin (NMuMG) supplemented with 10% fetal bovine serum, penicillin (100 IU/mL), and streptomycin (100 μg/mL) in a humidified atmosphere (37 °C and 5% CO_2).

2.4. Harvesting TA3/Ha and TA3-MTXR tumor cells

Mammary adenocarcinoma TA3/Ha ascites tumor cell line was grown by weekly intraperitoneal (i.p.) injection of 1.0×10^6 cells into young adult male CAF 1 Jax mice. TA3-MTXR methotrexate-resistant cell line was propagated in the same mouse strain (Araya-Maturana et al., 2002; Urra et al., 2013). Mice were housed and fed under the conditions previously described (Plaza et al., 2008), in the animal facility of Facultad de Medicina, Universidad de Chile. All the experiments were approved by two local ethics committees, from this Faculty and from the Comisión Nacional de Investigación Científica y Tecnológica (CONICYT). Tumor cells were harvested 5–7 days after i.p. inoculation of fluid from donor mice according to procedures described by us (Plaza et al., 2008).

2.5. Cellular respiration

Oxygen consumption was measured polarographically at 25 °C with a Clark electrode No. 5331 (Yellow Springs Instruments, Yellow Spring, OH, USA) using a YSI model 53 monitor, connected to a DI-148U data acquisition module with a USB interface. The data were obtained with Windaq Acquisition Waveform Recorder software (DataQ Instruments, USA). To characterize the mitochondrial metabolism of TA3/Ha cells, basal, ATP-linked, uncoupled and non-mitochondrial respiration were measured in two conditions: 1) only 4 mM glutamine and 2) 4 mM glutamine plus 5 mM glucose. TA3/Ha cells (5 mg protein/mL) were incubated in DMEM without glucose, L-glutamine and phenol red. Basal respiration was obtained from oxygen consumption rate (OCR) stimulated by addition of glutamine or glutamine plus glucose. Proton leak stimulated-respiration was obtained by 1 μM oligomycin addition and ATP synthesis-linked respiration was calculated by subtraction of proton leak stimulated respiration to basal respiration. Uncoupled and non-mitochondrial respirations were obtained by 200 nM carbonyl cyanide *m*-chlorophenylhydrazone (CCCP) and 1 μM antimycin A additions, respectively. All mitochondrial OCR values were calculated from non-mitochondrial OCR subtraction. To evaluate the effect of hydroquinones on cellular respiration, TA3/Ha cells (5 mg protein/mL) were incubated in RPMI-1640 without phenol red for 5 min and the respiration rates were registered in the absence (control in DMSO) or presence of hydroquinones for up to 30 min. The IC_{50} values were

calculated from the dose–response data of at least three independent experiments.

2.6. Isolation of mitochondria from tumor cells and rat liver

Mitochondria were isolated by fractional centrifugation from TA3/Ha ascites tumor cells permeabilized with digitonin as described by Moreadith and Fiskum (1984) and mitochondria from rat liver were isolated according to Ferreira (1990) and Pedersen et al. (1978) with modifications described by Plaza et al. (2008). In brief, each mitochondrial pellet was washed three times with their respective homogenization medium (pH, 7.2 and 7.4) in the absence of albumin to eliminate the adsorption of hydrophobic compounds (Plaza et al., 2008). Mitochondrial pellets were suspended to give a concentration of 40–50 mg protein/mL. Protein concentrations were determined by the Biuret reaction and standardized with albumin.

2.7. Mitochondrial respiration

Mitochondrial respiration was measured polarographically at 25 °C with a Clark electrode No. 5331 as described above (Urra et al., 2013). To determine the effect of selected compounds on the OXPHOS, mitochondria were stimulated with substrates for respiratory chain complex I (4.2 mM glutamate + 4.2 mM malate), complex II (5.0 mM succinate + 0.170 μM rotenone), complex III (0.30 mM duroquinol) and complex IV (1 μM antimycin + 0.075 mM TMPD + 1.5 mM ascorbate) in presence of ADP (0.25 mM), reaching state 3_{ADP}. To evaluate the effect of hydroquinone **9** on state 3u (CCCP-stimulated respiration) and state 4o (proton leak-driven respiration), 200 nM CCCP and 2 μM oligomycin were added, respectively. Respiratory Control Ratio (RCR) was calculated as the respiration in state 3_{ADP} divided by that in state 4. To evaluate the presence of cyanide-insensitive mitochondrial respiration, isolated mitochondria were stimulated sequentially with 5.0 mM succinate, 50 μM hydroquinone **9** and 250 μM KCN. To evaluate the participation of mPTP and ANT in the uncoupling effect induced by hydroquinone **9**, 1 μM cyclosporine A (CsA, with 2 min of incubation) and 30 μM atractyloside (Atrac) were used. To reverse the protonophoric effect of hydroquinone **9**, 100 μM 6-ketocholestanol was used.

2.8. Mitochondrial membrane potential in intact cells

Mitochondrial membrane potential ($\Delta\Psi m$) in intact cells was determined by flow cytometry using the potentiometric probe tetramethylrhodamine methyl ester (TMRM, Molecular Probe). Suspensions of TA3/Ha and NMuMG cells (1.5×10^5 cells/mL) were treated with DMSO (control) or 50 μM hydroquinone **9** for 2 h. CCCP (200 nM) was used as positive control. The cells were then washed with PBS and incubated with 50 nM TMRM for 20 min. Cells were collected, washed, re-suspended and fluorescence was detected using a BD FACSAria III flow cytometer.

2.9. Mitochondrial membrane potential in mitochondria isolated from TA3/Ha cells

In mitochondria isolated from TA3/Ha cells, $\Delta\Psi m$ was evaluated with the lipophilic cationic dye Rh123, following the protocol published by Wang et al. (2005). Unquenched fluorescence of this dye, which is released from mitochondria and indicative of the $\Delta\Psi m$, was quantified. 1.5-ml tubes were sequentially supplemented with 1 ml of mitochondrial buffer (Urra et al., 2013), substrate for complex I (4.2 mM glutamate + 4.2 mM malate) or complex II (5.0 mM succinate), 1 μM Rh123 and 0.5 mg/ml of mitochondrial suspension. Samples were incubated with DMSO (control), 200 nM CCCP, 1 μM rotenone or 50 μM hydroquinone **9**, for 10 min. Then, 0.2 mL aliquots of these reaction mixtures were transferred to a 96-well opaque assay plate and the unquenched fluorescence of the Rh123 dye was monitored using an 503/525 nm excitation/emission wavelength pair for a 5 to 25-min period using a varioSCAN fluorescence microplate reader.

2.10. Determination of intracellular ATP, NAD(P)H, glutathione and ROS levels

ATP levels were determined with CellTiter-Glo Luminescent Cell Viability Assay kit (Promega, USA) according to the manufacturer's specifications. TA3/Ha and NMuMG cells (1×10^5 cells/mL) were seeded into 96-well plates, incubating for 2 h in culture medium in the absence (control in DMSO) or presence of 50 μM hydroquinone **9**. After exposure, the cells were washed twice with PBS to remove the culture medium and re-suspended in 20 μL PBS. The bioluminescence was measured as described previously (Urra et al., 2013). Intracellular NAD(P)H levels were measured through auto-fluorescence. In brief, 5×10^5 cells/mL were seeded in 96-well plates and incubated in 100 μL PBS in the absence (control in DMSO) or presence of hydroquinone **9** (50 μM) for 15 min. Fluorescence was measured using an excitation wavelength of 340 nm and an emission wavelength of 428 nm. Folds change in NAD(P)H content was expressed with respect to the control (DMSO). Isocitrate (1 mM) was used to study the effect of hydroquinone **9** on NAD(P)H and glutathione levels, ROS and cell viability. Glutathione levels were expressed as GSH/GSSG ratio and were determined with Glutathione Fluorometric Assay kit (BioVision, USA) according to the manufacturer's specifications. The generation of intracellular oxidative stress was determined by spectrofluorometry using the 2′,7′-dichlorofluorescein diacetate (DCFH-DA) probe as described previously (Urra et al., 2013). TA3/Ha cells were incubated for 1 h with DMSO (control), 5 μM rotenone, and 50 μM hydroquinone **9**.

2.11. MTT assay and cell count

The MTT assay was used to evaluate cellular proliferation as described previously (Urra et al., 2013), seeding 1×10^4 cells/100 μL in 96-well microtiter plates and incubating for 24 h. The cells were then treated during 48 h with increasing concentrations of hydroquinones **9**, **14**, **17** and **18** (1, 5, 10, 50, 100 and 150 μM) to obtain a dose–response curve. The IC_{50} values were obtained from the dose–response data of at least three independent experiments. To evaluate the cell growth, TA3/Ha and NMuMG cells (25.000 cells) were seeded into 24-well plates and incubating for 24 h. Then, the cells were exposed for 24 and 48 h to DMSO (control), 50 μM hydroquinone **9**, 2.5 mM NAC, 2.5 mM isocitrate or in combination. After treatment, the cells were stained with a 0.4% solution of trypan blue in isotonic buffered salt solution and the number of cells was counted using a hemacytometer and optic microscopy. Doubling time was determined using the web-tool Doubling-time (Roth V. 2006; http://www.doubling-time.com/compute.php).

2.12. Cell cycle analysis

To estimate cell cycle distribution, cellular DNA contents were measured by flow cytometry as previously described (Urra et al., 2013). TA3/Ha cells were incubated with DMSO (control) or 50 μM hydroquinone **9** for 24 h. All samples were analyzed for cell cycle distribution using a FACS Calibur flow cytometer and the Becton–Dickinson CellQuest Acquisition software (San Jose, CA, USA). Data were reported as percentage of cells in each phase of the cell cycle.

2.13. Statistics

All statistical analyses were performed using Graph Pad Prism 4.03 (GraphPad Software, San Diego, California USA). The data are expressed as mean ± SEM of three independent experiments, each one performed in technical triplicate. Statistical analysis was performed using Student's *t*-test or one-way ANOVA with Bonferroni's post test for pairwise

comparisons. The data were considered statistically significant when $p < 0.05$.

3. Results

3.1. TA3/Ha cancer cells have a high mitochondrial metabolism

To characterize the mitochondrial metabolism of TA3/Ha cancer cells, the oxygen consumption in presence of glucose and glutamine as substrates was evaluated. TA3/Ha cells exhibited similar basal oxygen consumption rates (OCR) in these two conditions (Fig. 1A). The respiration was close to 68% oligomycin-sensitive in presence of glutamine or glutamine + glucose as substrates (Fig. 1C). Moreover, this effect also was observed at high glucose concentrations, indicating that cellular ATP is mainly produced by OXPHOS (data not shown). The maximum electron flow was evaluated using increased concentration of the uncoupler CCCP, the maximum OCR was reached to 200 nM (data not shown). TA3/Ha cells had a noteworthy high mitochondrial spare capacity (calculated from OCR in presence of CCCP–OCR in absence of CCCP), which was invariant in presence of glutamine or glutamine + glucose in saturating concentrations, suggesting that the maximal electron transport chain (ETC) activity can be stimulated independent of the glucose presence (Fig. 1D). These results indicate that glutamine is an important substrate for mitochondrial metabolism of TA3/Ha cells. Glutamine can be metabolized by enzymes as glutaminase and glutamate dehydrogenase (GDH) and alanine-leucine transaminase (ATL), converting α-ketoglutarate (DeBerardinis et al., 2007). To determine whether glutaminolysis is required to maintain the mitochondrial respiration, TA3/Ha cells were previously incubated with aminooxyacetic acid (AOA), an inhibitor of aminotransferase activity, and then exposed to glutamine or glutamine + glucose conditions. As Fig. 1E shows, the fully uncoupled mitochondrial respiration decreased in both conditions. These results indicate that glutamine is required for TCA cycle and production of substrates of ETC. On the other hand, the inhibition of electron flow by 1 μM antimycin-A addition completely reduced the oxygen consumption, indicating that the non-mitochondrial oxygen consumption (i.e. by presence of cytosolic oxidases) is minimal in both conditions (Fig. 1B). All together, these results indicate that TA3/Ha cancer cells have a high oxidative metabolism.

3.2. Identification of structural requirements of hydroquinones to affect respiration of TA3/Ha cells

Previously, hydroquinone **14** was identified, as an inhibitor of complex I-dependent respiration in TA3/Ha cancer cells (Urra et al., 2013). To determine the structural requirements to modulate the OXPHOS, a series of analogs of hydroquinone **14** were synthesized (Fig. 2A, compounds **15**–**22**). IC_{50} values shown that all hydroquinones analogs which have an increasing number of saturations relative to hydroquinone **14** (hydroquinones **20** and **22**), a methylene bridge (hydroquinone **15** and **21**), a 4-methylpent-3-en-1-yl chain (hydroquinone **16**), a *gem*-diethyl group (hydroquinone **19**) and hydroximethyl substitution (hydroquinones **17** and **18**) were between 2 to 10-folds less active than hydroquinone **14** in the inhibition of respiration (Supplementary Table 1). Moreover, we sought to determine the minimal structural characteristics required to affect the cellular respiration, evaluating the effect of bicyclic hydroquinones (**8**–**13**). All these hydroquinones were inactive (Table 1 and Supplementary Table 1). These results show that hydroquinone **14** is the best structure of this hydroquinone series to inhibit the respiration of TA3/Ha cancer cells.

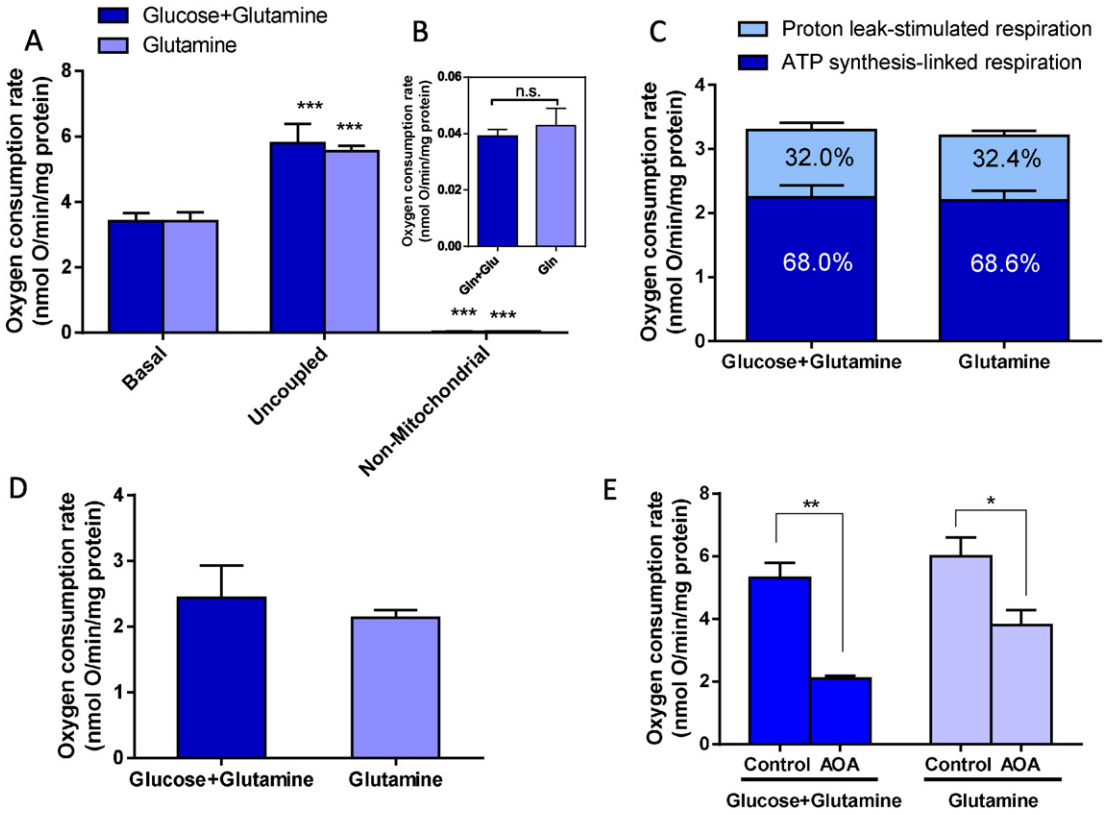

Fig. 1. Mitochondrial metabolism profile of TA3/Ha cancer cells. (A) Basal, uncoupled (addition of 200 nM CCCP) and non-mitochondrial respiration (1 μM antimycin-A), (B) inset, non-mitochondrial respiration, (C) participation of ATP synthesis and proton leak-stimulated respirations in basal respiration, (D) mitochondrial spare capacities in both conditions of substrates and (E) effect of inhibition of transaminase activity by 1 mM AOA in uncoupled respiration. Cells were exposed to glucose (5 mM) plus glutamine (2 mM), or only glutamine (2 mM). Data shown are the mean ± SEM of three independent experiments. n.s.: no significant, $^{***}p < 0.001$, $^{**}p < 0.01$ and $^{*}p < 0.05$ vs. basal respiration or control (DMSO), in A and E, respectively.

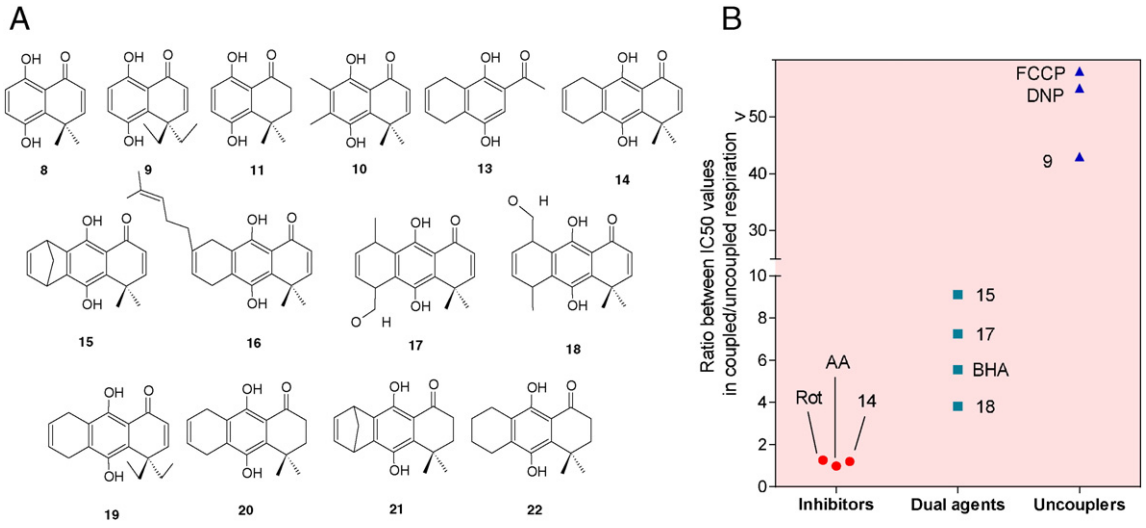

Fig. 2. Structural changes on hydroquinone scaffold produce compounds with different actions on OXPHOS. (A) Chemical structures of *ortho*-carbonyl substituted hydroquinones. The syntheses are described in the supplementary section. (B) Ratio of IC_{50} values of compounds in coupled/uncoupled respiration in TA3/Ha cells. Rot: rotenone, AA: antimycin-A, BHA: t-butyl-4-hydroxyanisole, DNP: 2,4-dinitrophenol and FCCP: carbonyl cyanide-4-(trifluoromethoxy)phenylhydrazone.

3.3. Dependence of the action of hydroquinones on the uncoupled and coupled respiration in TA3/Ha cells

To determine the effect of the analogs of hydroquinone **14** on the electron transport chain (ETC) and its dependence on the coupling of OXPHOS, TA3/Ha cells were incubated with protonophoric mitochondrial uncoupler CCCP (Table 1, +CCCP) and the effect on OCR was evaluated. As Table 1 shows, the hydroquinones exhibited different inhibitory activities on coupled and uncoupled respiration. Hydroquinone **14**, exhibited a ratio −CCCP/+CCCP = 1.26, indicating that the action is independent of the status of coupling of OXPHOS. Similar values were also obtained with well-known mitochondriotoxic compounds (Fig. 1B): complex-I inhibitor rotenone (IC_{50} −CCCP = 0.125 μM and IC_{50} + CCCP = 0.105 μM) and complex-III inhibitor antimycin-A (IC_{50} −CCCP = 0.656 μM and IC_{50} + CCCP = 0.669 μM) exhibited a ratio −CCCP/+CCCP = 1.18 and 0.98, respectively. In contrast, hydroquinones **15**, **17** and **18** exhibited a intermediate ratio −CCCP/+CCCP between 3.82–9.11, similar to t-butyl-4-hydroxyanisole (BHA: IC_{50} −CCCP = 0.943 mM and IC_{50} + CCCP = 0.170 mM; ratio −CCCP/+CCCP = 5.55), which is a reported compound with uncoupling effect of OXPHOS at low concentrations and inhibitory effect of mitochondrial respiration at high concentrations (Ferreira, 1990; Lou et al., 2007). These intermediate values of the ratio −CCCP/+CCCP suggest that these hydroquinones can be dual agents with uncoupling and inhibitory effects on OXPHOS. Finally, very high or undeterminable ratio −CCCP/+CCCP were obtained for the uncoupling agents 2,4-dinitrophenol (DNP) and carbonyl cyanide-4-(trifluoromethoxy)phenylhydrazone (FCCP). These results indicate that they do not inhibit the respiration, being the main effect the uncoupling of OXPHOS. Interestingly, hydroquinone **9** exhibited the highest difference in IC_{50} values (Table 1), suggesting to be an uncoupler. Other bicyclic and tricyclic hydroquinones were inactive in presence and absence of CCCP (data not shown). Because that these small structural changes produced different actions on OXPHOS compared to hydroquinone **14**, hydroquinone **9** was selected to evaluate this hypothesis in the follow sections.

Table 1
Inhibitory effect of *ortho*-carbonyl substituted hydroquinones on the respiration of TA3/Ha cells. IC_{50} values are the mean of three different experiments ± SEM, expressed as mM. ([c]) IC_{50} values are from Urra et al. (2013).

Cpd.	IC_{50} (−) CCCP	IC_{50} (+) CCCP	Ratio (−) CCCP/(+) CCCP
9	0.43 ± 0.04	0.01 ± 0.03	43.00
14[c]	0.082 ± 0.013	0.065 ± 0.027	1.26
15	0.856 ± 0.040	0.094 ± 0.050	9.11
17	0.29 ± 0.02	0.040 ± 0.002	7.25
18	0.420 ± 0.020	0.110 ± 0.030	3.82

3.4. Hydroquinone 9 uncouples OXPHOS in mitochondria isolated from TA3/Ha cells

Hydroquinone **9** increased the mitochondrial respiration in presence of ADP (Fig. 3A) and decreased the Respiratory Control Ratio (RCR), when complex I- or II-dependent respirations were stimulated (Fig. 3B), suggesting that it produces a total uncoupling of OXPHOS in mitochondria isolated from TA3/Ha cells. At 50 μM, hydroquinone **9** produced a RCR value close to 1, independent the respiratory complex stimulated (Fig. 3B). To evaluate the effect of hydroquinone **9** on ATP synthesis-linked respiration (state 3_{ADP}), specific substrate were used to stimulate each respiratory complexes in the presence of ADP. None inhibitory effect was observed when complexes I, II, III and IV were stimulated in presence of hydroquinone **9** (Fig. 3C), suggesting that this compound does not affect the ATP synthesis-linked respiration, without produce inhibition of respiratory complexes. On the other hand, hydroquinone **9** causes an increase of the mitochondrial respiration in state 4o to 1.934 ± 0.108-folds compared with the control ($p < 0.001$; Fig. 3D) and decreases the uncoupled respiration (state 3u) to 1.284 ± 0.165-folds, suggesting that this compound produces an ΔΨm-dependent increase of the proton leak across the inner mitochondrial membrane. Interestingly, hydroquinone **9** exhibited a little effect on respiration of mitochondria isolated from rat liver. It slightly decreases the RCR at 50 μM ($p < 0.01$; Fig. 4A), producing an increase of mitochondrial respiration in state 4 to 1.26 ± 0.04-folds of control ($p < 0.05$), without effects on mitochondrial respiration in state 3_{ADP} (Fig. 4B–C). Collectively, these results indicate that hydroquinone **9** produces selective and total uncoupling of OXPHOS in TA3/Ha cells.

3.5. Hydroquinone 9 uncouples OXPHOS through a protonophoric mechanism

To determine the mechanism of the uncoupling effect produced by hydroquinone **9**, to mitochondria in state 2 incubated with cyclosporine and atractyloside, inhibitors of mPTP and ANT, respectively, were added hydroquinone **9** and the OCR was measured. No significant effects were detected (Fig. 5A–C). To evaluate if the increase in the mitochondrial respiration produced by hydroquinone **9** is due an increase in the

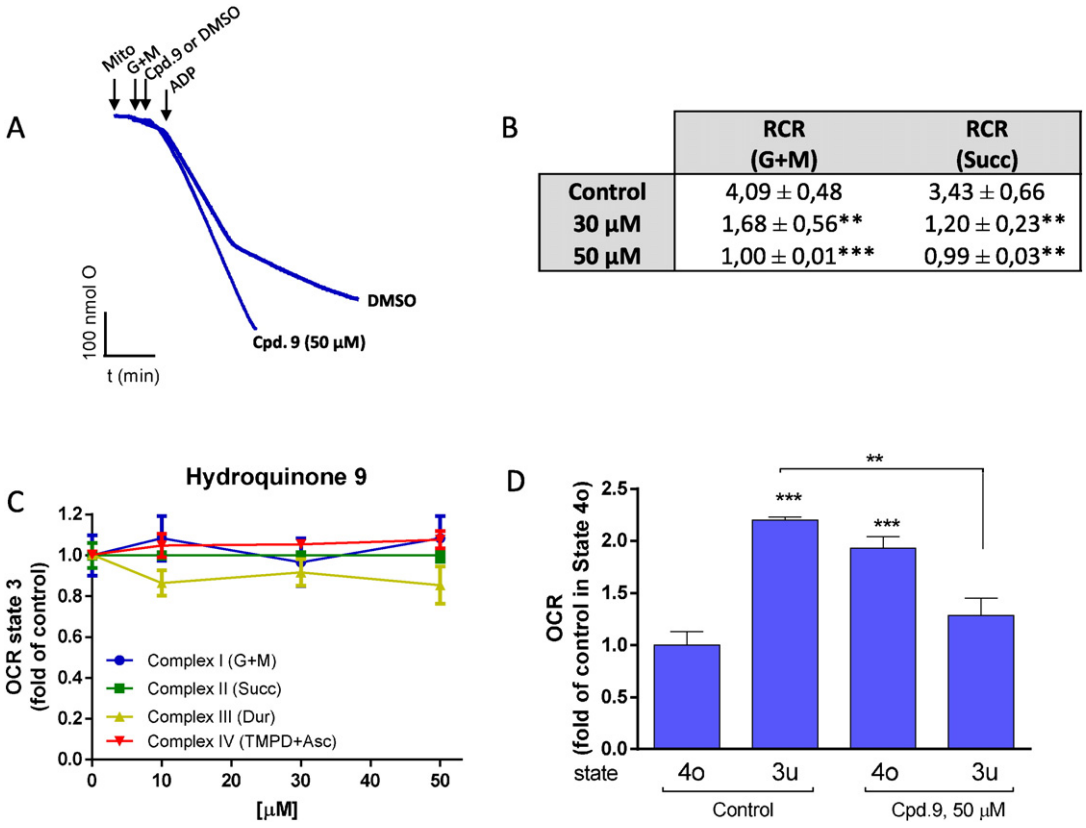

Fig. 3. Effect of hydroquinone **9** on OXPHOS. (A) Representative traces of oxygen consumption rate in mitochondria isolated from TA3/Ha cells in presence of hydroquinone **9** or DMSO (control); (B) effect on Respiratory Control Ratio (RCR) when respiratory complexes I and II are stimulated with glutamate plus malate or succinate, respectively; (C–D) effect of hydroquinone **9** on mitochondrial respiration in state 3_{ADP}, state 3u and state 4o. Respiratory Control Ratio (RCR) was calculated as the respiration in state 3_{ADP} divided by that in state 4. Data shown are the mean ± SEM of three independent experiments. $^{**}p < 0.01$, $^{***}p < 0.001$, vs. control (DMSO).

oxygen consumption by ETC, KCN was added to mitochondria in the presence of hydroquinone **9**. As Fig. 5D shows, KCN addition blocked the oxygen consumption, suggesting that this compound requires a functional ETC. In addition, when 6-ketocholestanol (6-keto), a keto-derivative of cholesterol that decreases the membrane fluidity (Chávez et al., 1996; Cuéllar et al., 1997), was added in the presence of hydroquinone **9**, mitochondrial respiration was normalized (hydroquinone **9**: 2.743 ± 0.063-folds increase vs. hydroquinone **9** + 6-keto: 0.916 ± 0.018-fold increases, both with respect to control), similar to state 2 (Fig. 5E,G), suggesting that membrane fluidity is required to increase the mitochondrial respiration by this hydroquinone. The same reversion was obtained for known protonophore CCCP (Fig. 5F, Starkov et al., 1994). Moreover, changes in ΔΨm maintained by complex I- and complex II-dependent respiration (state 2) in isolated mitochondria were evaluated. Hydroquinone **9**, similar to CCCP, decreases ΔΨm independently of mitochondrial substrate used (Fig. 5H); in contrast to rotenone, a complex I-inhibitor, only produced a decrease of ΔΨm when isolated mitochondria were incubated with glutamate plus malate. Taken together, this evidence suggests that hydroquinone **9** is a protonophoric uncoupler of OXPHOS.

3.6. Hydroquinone 9 produces mitochondrial dysfunction in TA3/Ha cancer cells

Hydroquinone **9** reduces the mitochondrial spare capacity (Fig. 6A), decreases the ATP levels and ΔΨm at 2 h of exposition (Fig. 6B–C) and it also produces an increase of intracellular ROS levels (Fig. 6D), but without detectable mitochondrial superoxide production in intact TA3/Ha cells (Supplementary Fig. 2A). In mouse mammary epithelial cells NMuMG, this compound does not affect the ATP levels and ΔΨm (Fig. 6B–C). These results indicate that hydroquinone **9** selectively produces bioenergetic dysfunction in TA3/Ha cells. Consistent with the above, this compound decreased the NAD(P)H levels to 0.625 ± 0.063 folds of the control ($p < 0.001$, Fig. 6E) in TA3/Ha cells without affect the NAD(P)H levels in NMuMG cells (Fig. 6E). NAD(P)H levels are maintained by TCA cycle and required for ATP synthesis by OXPHOS and regeneration of antioxidant gluthatione system (Stein and Imai, 2012; Alberghina and Gaglio, 2014). In TA3/Ha cells, hydroquinone **9** decreased the GSH/GSSG ratio after 24 h of exposition (Fig. 7F) and the addition of 1 mM isocitrate, a substrate of isocitrate dehydrogenases, reversed the effect of hydroquinone **9** on NAD(P)H levels ($p < 0.01$, Fig. 6E) and GSH/GSSG ratio ($p < 0.05$, Fig. 6F). These results suggest that hydroquinone **9** produces mitochondrial dysfunction with changes in the NAD(P)H availability, affecting the redox status in TA3/Ha cells.

3.7. Hydroquinone 9 has NAD(P)H availability-dependent anti-proliferative effects on cancer cells

To evaluate if the alterations induced in OXPHOS by hydroquinone **9** affect the viability of cancer cells, sub-G1 population was evaluated in TA3/Ha cells. Hydroquinone **9** did not affect the cell viability (Supplementary Fig. 2C); however, it produced alteration in the cell cycle distribution, arresting in G2/M-phase at 24 h (Fig. 7A–C). To evaluate if this affects the cell growth, the effect of hydroquinone **9** on the number of NMuMG epithelial cells and TA3/Ha cancer cells was determined at 24 and 48 h. Hydroquinone **9** inhibited selectively the growth of TA3/Ha cells (Fig. 7E and G). Consistently, as Fig. 7F and H, show this compound produced an increase in the doubling time of TA3/Ha cancer cell (control: 26.00 ± 1.85 h vs hydroquinone **9**: 74.18 ± 5.26 h, $p < 0.001$) without modifying that of NMuMG epithelial cells (control: 25.54 ± 2.27 h vs hydroquinone **9**: 27.80 ± 3.15 h). Moreover, this decreased number of TA3/Ha cells produced by hydroquinone **9** at 48 h of exposition was

A

	RCR (G+M)
Control	3,49 ± 0,22
10 μM	3,96 ± 0,80
30 μM	3,17 ± 0,12
50 μM	2,19 ± 0,08**

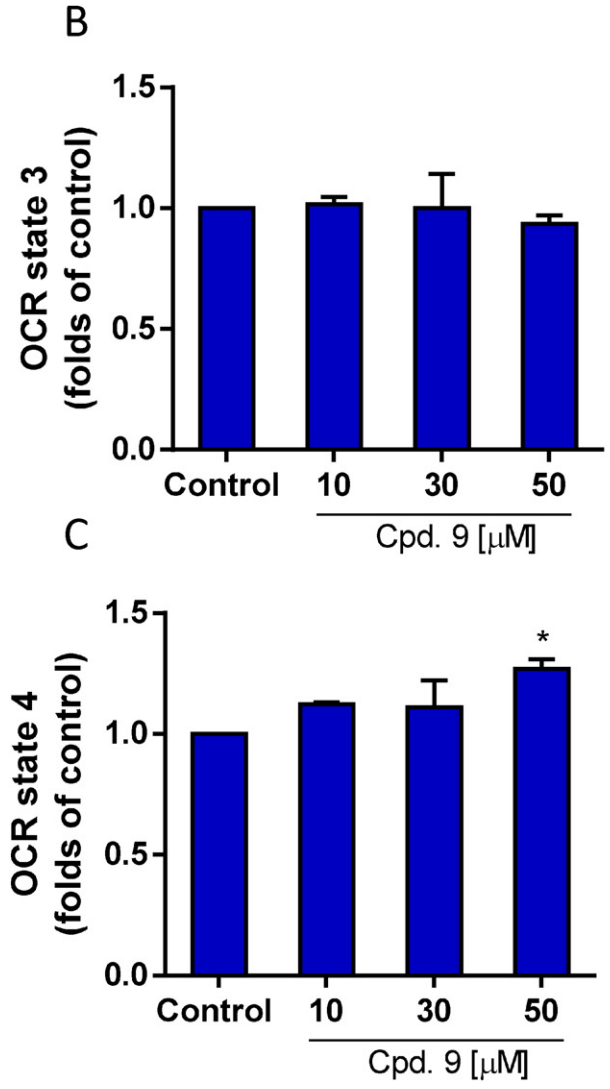

Fig 4. Hydroquinone **9** slightly affects the respiration of mitochondria isolated from rat liver. Effect of hydroquinone **9** on (A) Respiratory Control Ratio (RCR) and (B–C) mitochondrial respiration in state 3_{ADP} and state 4. Substrates added were glutamate plus malate (G + M). Respiratory Control Ratio (RCR) was calculated as the respiration in state 3_{ADP} divided by that in state 4. Data shown are the mean ± SEM of three independent experiments. $^{**}p < 0.01$, $^{*}p < 0.05$, vs. control (DMSO).

reversed by isocitrate and NAC combination (Fig. 7D). Collectively, these results indicate that changes in the NAD(P)H availability produced by hydroquinone **9** selectively affect the proliferation of TA3/Ha cells. On the other hand, hydroquinone **9** shows an anti-proliferative effect in murine (TA3/Ha and the methotrexate-resistant variant TA3-MTXR) and human (CCRF-CEM and the camptothecin-resistant variant CEM/C2) cancer cells (Table 2). In leukemic CCRF-CEM cells, this hydroquinone produces similar bioenergetic alterations to those described in TA3/Ha cells, affecting the oxygen consumption (data not shown), NAD(P)H and ATP levels (Supplementary Fig. 3). Moreover, hydroquinone **9** did not affect the proliferation of non-malignant MM3MG cells, suggesting a selective anti-proliferative effect on cancer cells. Comparisons between cancer cell lines and their resistant variants indicate that hydroquinone **9** presents a relative resistance index (RRI) close to 1 (calculated as the IC_{50} drug resistant cells/IC_{50} drug sensitive cells ratio, Table 2), similar to previously reported hydroquinone **14** (Urra et al., 2013).

4. Discussion

4.1. Characteristics on mitochondrial metabolism of TA3/Ha cells and implications in anti-cancer evaluations

We describe here for first time the effect of glutamine and glucose on mitochondrial metabolism of TA3/Ha cells, which is an ascites tumor cell line. The mitochondrial respiration in basal conditions, in the presence of glutamine or glutamine plus glucose, was 68% inhibited by addition of oligomycin, suggesting ATP's pool that supports the cellular requirements mainly proceed from OXPHOS. Differences between the maximal electron flow, which is obtained in an uncoupled respiration, and respiration in basal conditions, reflect the bioenergetics status of the mitochondria, being a spare capacity to response to energy demand or some metabolic stress (Hill et al., 2012). This spare capacity is occupied in a 62% in basal conditions, a characteristic that was independent from the oxidized substrate. It has been described that ascites liquid exhibits high concentrations of oxygen and glutamine with very low concentration of glucose (Rodríguez-Enríquez et al., 2000). Consequently, no detectable differences between the respiration in presence of glutamine or glutamine plus glucose were observed in TA3/Ha cells, suggesting that glutamine is a preferential substrate for mitochondrial metabolism of TA3/Ha cells. Interestingly, glutamine, similar to glucose, is metabolized in several pathways that support bioenergetics, biosynthesis and proliferation in some cancer cells (DeBerardinis et al., 2007). Glutamine can be converted to α-ketoglutarate (α-KG) by enzymes as glutamate dehydrogenase (GDH) and alanine-leucine transaminase (ATL), serving as anaplerotic precursors (DeBerardinis et al., 2007). In TA3/Ha cells, addition of aminooxyacetic acid (AOA), inhibitor of aminotransferase activity, decreased the oxygen consumption when CCCP was added in the presence of both glutamine and glutamine plus glucose, indicating that intermediates of TCA cycle and substrate of ETC derived from glutaminolysis.

Several type of human cancer cells exhibit a high mitochondrial metabolism (Moreno-Sánchez et al., 2014). Then, the modulation of mitochondrial respiration to produce mitochondrial dysfunction results in a strategy for targeting these cancer cells (Fantin et al., 2002; Cheng et al., 2013; Zhang et al., 2014). Here, we used TA3/Ha cells as model for studying the mechanism of action of the hydroquinone analogs on OXPHOS in cancer cells. Interestingly, similar effects to those described in TA3/Ha cells on mitochondrial bioenergetics and proliferation were observed in CCRF-CEM human leukemic cells. Moreover, the proliferation of resistant variants to chemotherapeutics of these cell lines was also affected by the hydroquinone analogs. Consistent with this, it has been recently reported the selective cytotoxic effects of *ortho*-acylated-1,4-naphthohydroquinones by a mechanism of mitochondria-mediated cell death on a panel of leukemia cells (Pedroza et al., 2014). This suggests that the hydroquinone scaffold can offer a possibility to obtain compounds with selective anti-cancer effect, especially in lymphoma or leukemia cells, which have a high mitochondrial participation in the energetic metabolism (Jitschin et al., 2014; Yizhak et al., 2014).

4.2. Structural relationship between hydroquinone scaffold and mitochondrial respiration

Structural factors of known inhibitors of complex I required to interact with this enzyme are not obvious, being different in each inhibitor type (Miyoshi, 2001). Generally, these compounds exhibit aromatic

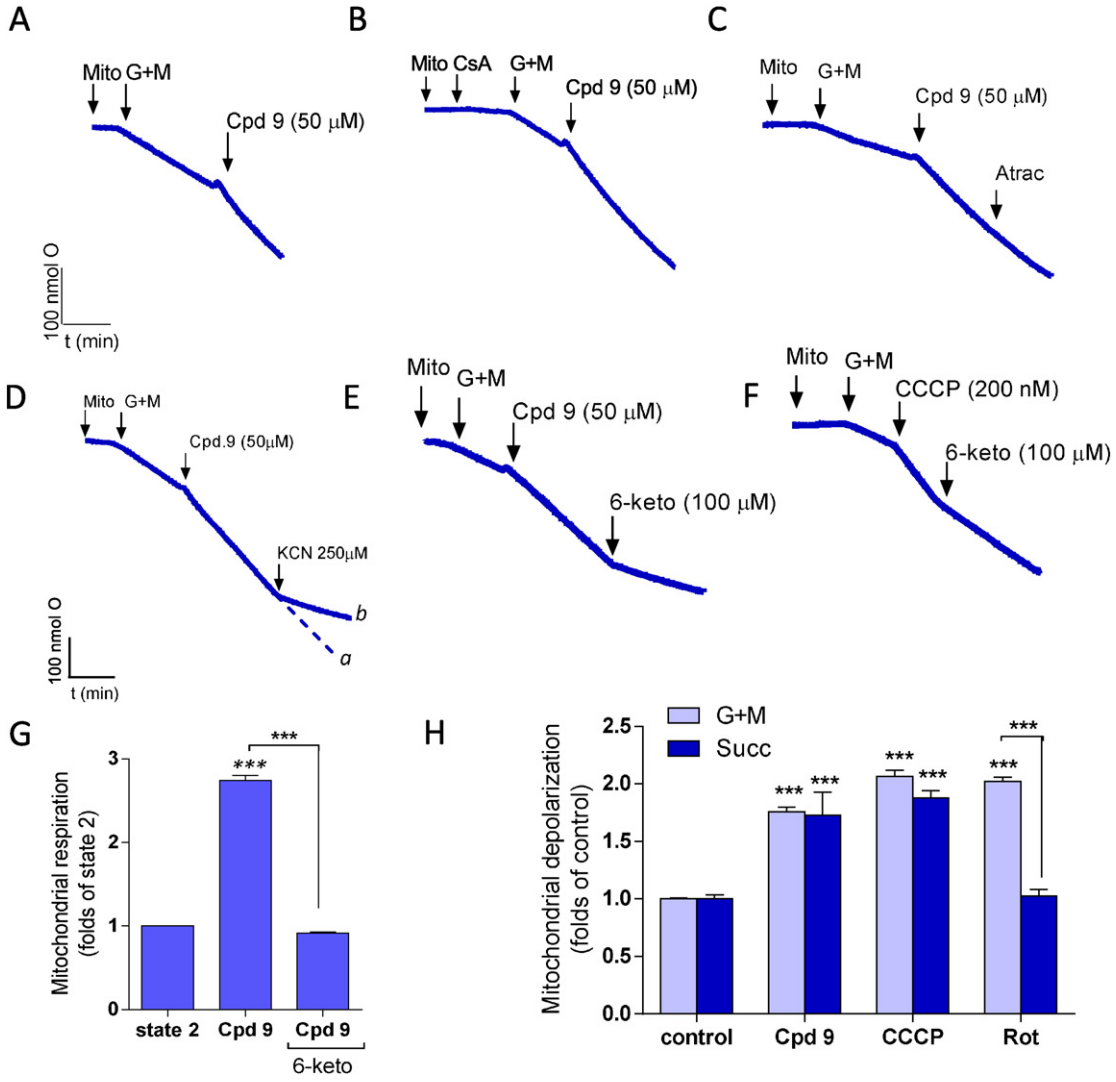

Fig. 5. Hydroquinone **9** is a protonophoric uncoupler of OXPHOS. (A) Effect of hydroquinone **9** on mitochondrial respiration in state 2. (B) Increase of oxygen consumption produced by hydroquinone **9** does not involve opening of permeability transition pore (PTP), (C) activation of ANT and (D) redox cycling. (E–G) 6-ketocholestanol (6-keto) reverses uncoupling effect produced by 50 μM hydroquinone **9** and 200 nM CCCP. Mitochondria (0.5 mg/mL) and glutamate + malate (G + M) were added as indicated by the arrows. CsA, cyclosporin A; Atrac, atractyloside. Oxygen consumption was determined by Clark oxygen electrode. (H) Mitochondrial depolarization produced by 50 μM hydroquinone **9**, 200 nM CCCP and 1 μM rotenone when complex I (G + M: glutamate plus malate) and complex II (Succ: succinate) are stimulated. Data shown are the mean ± SEM of three independent experiments. $^{***}p < 0.001$, vs. control (DMSO).

rings with a hydroquinone/quinone motif, showing planarity in its geometrical requirements (Okun et al., 1999) and its interaction with complex I is highly sensitive to structural changes (Ueno et al., 1994; Satoh et al., 1996). Our results indicate that the *ortho*-carbonyl substituted hydroquinone **14** represents the minimum structure that fulfills the molecular requirements to inhibit cellular respiration in cancer cells by interaction with complex I. Interestingly, the incorporation of a methylene bridge and different substituents on the scaffold of hydroquinone **14** decreased its inhibitory effect, affecting the interaction with complex I; however, these structural modifications generated compounds with other effects on OXPHOS. As previously reported, hydroquinone **14** produces inhibition of complex I-dependent respiration (Urra et al., 2013) and this effect is independent of the status of coupling of OXPHOS (this study), similar to rotenone and antimycin-A, complex I and III inhibitors respectively. Interestingly, analogs of hydroquinone **14** with substitutions located in the hydroquinone plane exhibited a dual mechanism of action on cellular respiration with anti-proliferative effects (Supplementary Figs. 2 and 3). At low concentrations, they produced uncoupling of OXPHOS through a protonophoric mechanism and only at high concentrations retained the interaction with complex I, inhibiting only mitochondrial respiration stimulated by glutamate plus malate (Supplementary Fig. 4). These effects also were observed on RCR when complexes I and II were stimulated (Supplementary Fig. 4). Dual effects have been previously reported for other compounds like BHA (Ferreira, 1990; Lou et al., 2007). These compounds primarily increase oxygen consumption rate producing uncoupling by several mechanisms, being suggested that inhibition of ETC or mitochondrial ATP synthesis is a secondary effect (Lou et al., 2007). Consistent with this, the dual agents exhibited an intermediate ratio IC_{50} −CCCP/+CCCP between 3.82–9.11. On the other hand, bicyclic hydroquinones were inactive on respiration, except hydroquinone **9** which had a ratio IC_{50} −CCCP/+CCCP = 43.00, suggesting that its effect is dependent of coupling of OXPHOS. Interestingly, this compound increased the proton leak-stimulated respiration in isolated mitochondria by a protonophoric mechanism, i.e. hydroquinone **9** may act as a proton shuttle, transporting protons across mitochondrial membrane, dissipating the proton gradient leading to uncoupling of the ADP phosphorylation from the electron transport and hydrogen transfer in ETC. It is known that physico-chemical properties, such as lipophilicity and acidity, are important factors for uncoupling of OXPHOS by protonophore agents (Spycher et al., 2008; Naven et al.,

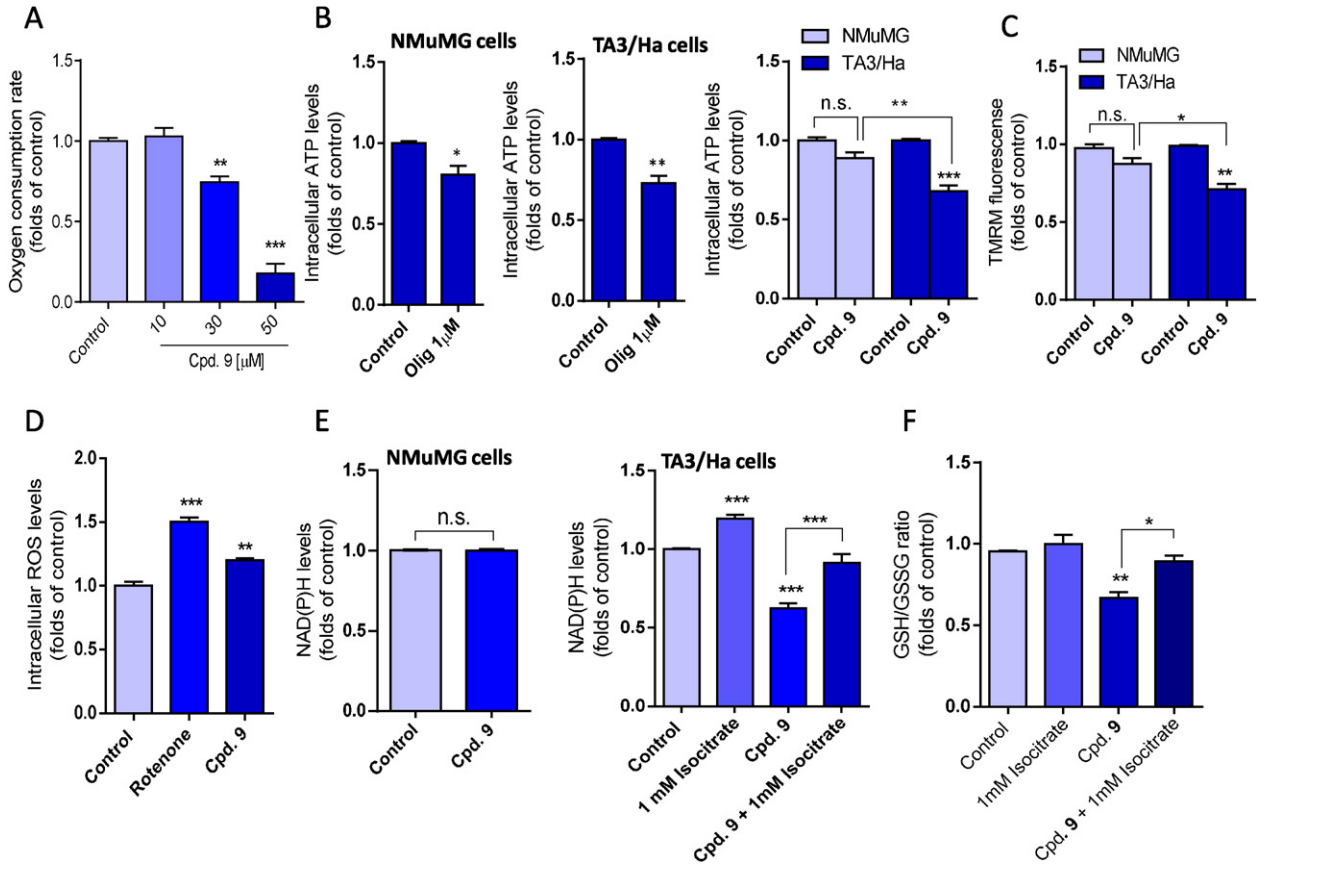

Fig. 6. Hydroquinone **9** produces mitochondrial dysfunction in TA3/Ha cells. Effects of hydroquinone **9** (50 μM) on (A) mitochondrial spare capacity in TA3/Ha cells, (B) intracellular ATP levels and (C) mitochondrial transmembrane potential in TA3/Ha and NMuMG cells, (D–F) intracellular ROS production, NAD(P)H levels and GSH/GSSG ratio in TA3/Ha cells. Data shown are the mean ± SEM of three independent experiments. $^{***}p < 0.001$, $^{**}p < 0.01$ and $^{*}p < 0.05$ vs. control (DMSO).

2013). Previously, we reported a theorical study on factors that affect the capability of the bicyclic hydroquinones to cross membranes, where the phenol-phenoxide equilibrium and the solvation energy of neutral species were evaluated (Soto-Delgado et al., 2013). It is possible that a similar mechanisms occurs with hydroquinone **9**, being the translocation rate of the charged species a limiting step, as previously reported for other uncouplers (Spycher et al., 2008). Moreover, the intramolecular hydrogen bond between the phenolic hydrogen and the oxygen from the *orto*-carbonyl motif (Martínez-Cifuentes et al., 2014) can involve a change in the acidity of the protonophore motif, increasing its ability to act as uncoupler. These results suggest that the planarity of hydroquinone **14** scaffold is essential for the interaction with the ETC, and when this scaffold is chemically substituted an uncoupling effect is primary evident.

*4.3. Effect of hydroquinone **9** on mitochondrial bioenergetics and proliferation of cancer cells*

Isolated mitochondria are considered the best approach for studies about mechanisms (Brand and Nicholls, 2011). Moreover, tumor and non-malignant mitochondria exhibit differences at the OXPHOS level (Solaini et al., 2011; Panov and Orynbayeva, 2013), and mitochondria isolated from different tissues are differentially affected by small molecules (Baliutyte et al., 2010). In this sense, several studies on the mechanism of action of anti-cancer compounds have been made on mitochondria isolated from non-malignant tissue (Fantin et al., 2002; Filomeni et al., 2009; Pardo-Andreu et al., 2011). In this study, mitochondria isolated from adenocarcinoma cells were used to maintain the biochemical characteristics of tumor mitochondria and reveal the impact of hydroquinones on OXPHOS in these organelles. Hydroquinone **9** produced total uncoupling of OXPHOS only in mitochondria isolated from TA3/Ha cells, with less effect on respiration of mitochondria isolated from rat liver, suggesting a selective effect on bioenergetics of cancer cells. Consistently, it decreased the ΔΨm, ATP and NAD(P)H levels in TA3/Ha intact cells, producing mitochondrial dysfunction (Fig. 7I). Mitochondrial control of NAD^+/NADH and $NADP^+$/NADPH levels is maintained by nicotinamide nucleotide transhydrogenase, a ΔΨm-dependent enzyme that resides in the inner mitochondrial membrane (Gameiro et al., 2013), whose activity is sensitive to uncouplers (Rydström, 2006). Hydroquinone **9** produced a decrease of intracellular NAD(P)H levels in murine and human cancer cells, which was an important event that affected the proliferation. This effect was reversed by isocitrate, an essential intermediate of several biochemical pathways, including TCA cycle (Icard et al., 2012). These results suggest that uncoupling of OXPHOS induced by hydroquinone **9** can deplete the intermediates of the TCA cycle, such as isocitrate and reduced equivalents (NAD(P)H). This is affecting not only mitochondrial ATP synthesis, but also other pathways that use NADPH as cofactor to maintain the redox balance by reduced glutathione, and probably the biosynthesis of fatty acids, nucleotides and amino acids, which promote proliferation of cancer cells. Interestingly, FCCP and 2,4-dinitrophenol, known protonophoric uncouplers, induce cell cycle arrest in G1-phase and apoptosis in cancer cells by increase of ROS levels with depletion of GSH content (Han et al., 2008, 2009). Similar effects on redox status were detected in TA3/Ha cells treated with hydroquinone **9**, however, apoptotic populations were not detectable after 24 h of exposition. This evidence supports the idea that a decrease in the NAD(P)H availability by uncoupling of OXPHOS, represents a major impact on malignant cells, accounting for the high selectivity exhibited by hydroquinone **9** on cell proliferation.

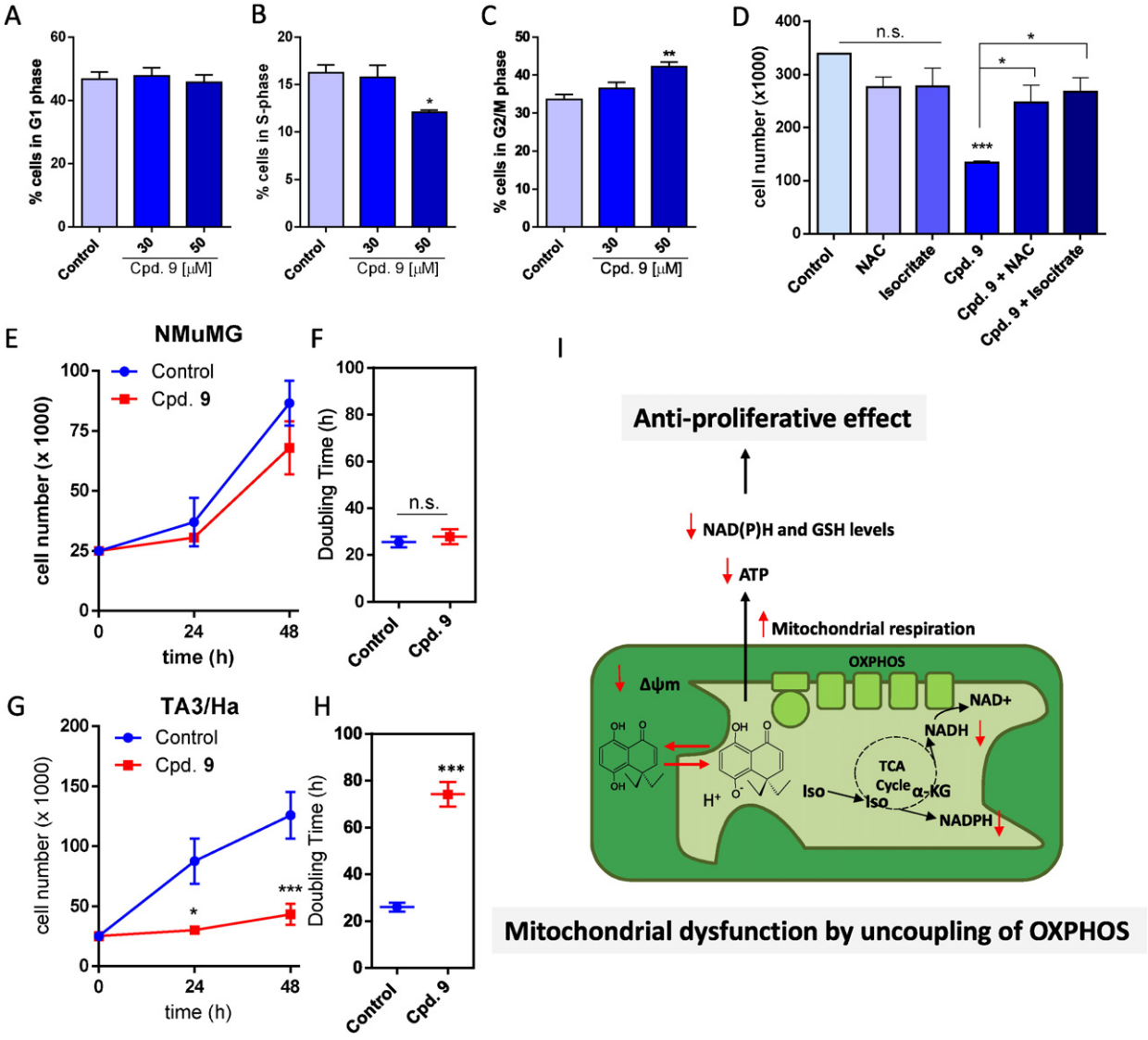

Fig. 7. Hydroquinone **9** selectively decreases the proliferation of TA3/Ha cells. Effect of hydroquinone **9** on (A–C) cell cycle distribution and (D) number of TA3/Ha cells at 24 h and 48 h of exposition, respectively. Effect of hydroquinone **9** on cell growth and doubling time of (E–F) NMuMG and (G–H) TA3/Ha. (I) Mechanism of action proposed for hydroquinone **9**. Iso: isocitrate, α-KG: alpha-ketoglutarate, ΔΨm: mitochondrial membrane potential. Data shown are the mean ± SEM of three independent experiments. $^{***}p < 0.001$, $^{**}p < 0.01$ and $^{*}p < 0.05$ vs. control (DMSO).

In conclusion, our results show that small structural changes on the scaffold of *ortho*-carbonyl substituted hydroquinone **14** allow to obtain specific mechanisms of action on OXPHOS by inhibition of complex I-dependent respiration, uncoupling of OXPHOS or compounds with both actions, affecting the proliferation of cancer cells with high oxidative metabolic phenotype. This provides useful evidence to design new anti-cancer compounds.

Table 2
Anti-proliferative effect of Cpd. **9** and Cpd. **14** on cancer and non-malignant cells and resistance index (RRI). The IC_{50} values are the mean of three different experiments ± SEM. RRI was calculated for murine and human cancer cells as the IC_{50} drug resistant cells/IC_{50} drug sensitive cells ratio. ([c]) IC_{50} and RRI values are from Urra et al. (2013).

	Cpd. 9		Cpd. 14	
	IC_{50} [μM]	RRI	IC_{50} [μM]	RRI
MM3MG	>100	–	90.48 ± 4.29[c]	–
NMuMG	73.55 ± 3.20	–	>100	–
TA3/HA	24.34 ± 2.00	1.08	13.00 ± 3.58[c]	1.06
TA3-MTXR	26.38 ± 0.77		12.90 ± 0.84[c]	
CCRF-CEM	27.77 ± 0.96	1.00[c]	13.05 ± 2.50	1.08
CEM/C2	25.83 ± 1.01		14.14 ± 4.25	

Transparency document

The Transparency document associated with this article can be found, in the online version.

Conflict of interest statement

The authors have no conflicts of interest to declare.

Acknowledgments

This work was supported by FONDECYT grants 1110176, 1140753 and 1130772 and ACT 1107. FAU, MC-D and MM-C thank CONICYT for PhD fellowships. ORR and ML thank FONDECYT postdoctoral grant 3120235 and 3160022, respectively.

Appendix A. Supplementary data

Supplementary data to this article can be found online at http://dx.doi.org/10.1016/j.taap.2015.12.005.

References

Alberghina, L., Gaglio, D., 2014. Redox control of glutamine utilization in cancer. Cell Death Dis. 5, e1561.

Araya-Maturana, R., Cardona, W., Cassels, B.K., Delgado-Castro, T., Ferreira, J., Miranda, D., Pavani, M., Pessoa-Mahana, H., Soto-Delgado, J., Weiss-López, B., 2006. Effects of 9,10-dihydroxy-4,4-dimethyl-5,8-dihydro-1(4H)-anthracenone derivatives on tumor cell respiration. Bioorg. Med. Chem. 14, 4664–4669.

Araya-Maturana, R., Cassels, B.K., Delgado-Castro, T., Valderrama, J.A., Weiss-López, B.E., 1999. Regioselectivity in the Diels–Alder reaction of 8,8-dimethylnaphthalene-1,4,5(8H)-trione with 2,4-hexadien-1-ol. Tetrahedron 55, 637–648.

Araya-Maturana, R., Delgado-Castro, T., Gárate, M., Ferreira, J., Pavani, M., Pessoa-Mahana, H., Cassels, B.K., 2002. Effects of 4,4-dimethyl-5,8-dihydroxynaphtalene-1-one and 4,4-dimethyl-5,8-dihydroxytetralone derivatives on tumor cell respiration. Bioorg. Med. Chem. 10, 3057–3060.

Baliutyte, G., Baniene, R., Trumbeckaite, S., Borutaite, V., Toleikis, A., 2010. Effects of *Ginkgo biloba* extract on heart and liver mitochondrial functions: mechanism(s) of action. J. Bioenerg. Biomembr. 42, 165–172.

Barbi de Moura, M., Vincent, G., Fayewicz, S.L., Bateman, N.W., Hood, B.L., Sun, M., Suhan, J., Duensing, S., Yin, Y., Sander, C., Kirkwood, J.M., Becker, D., Conrads, T.P., Van Houten, B., Moschos, S.J., 2012. Mitochondrial respiration — an important therapeutic target in melanoma. PLoS One 7, e40690.

Bellance, N., Benard, G., Furt, F., Begueret, H., Smolková, K., Passerieux, E., Delage, J., Baste, J., Moreau, P., Rossignol, R., 2009. Bioenergetics of lung tumors: alteration of mitochondrial biogenesis and respiratory capacity. Int. J. Biochem. Cell Biol. 41, 2566–2577.

Brand, M.D., Nicholls, D.G., 2011. Assessing mitochondrial dysfunction in cells. Biochem. J. 435, 297–312.

Chávez, E., Moreno-Sánchez, R., Zazueta, C., Cuéllar, A., Ramirez, J., Reyes-Vivas, H., Bravo, C., Rodríguez-Enríquez, S., 1996. On the mechanism by which 6-ketocholestanol protects mitochondria against uncoupling-induced Ca^{2+} efflux. FEBS Lett. 379, 305–308.

Chen, G., Zhang, X., Zhao, M., Wang, Y., Cheng, X., Wang, D., Xu, Y., Du, Z., Yu, X., 2011. Celastrol targets mitochondrial respiratory chain complex I to induce reactive oxygen species-dependent cytotoxicity in tumor cells. BMC Cancer 11, 170.

Cheng, G., Zielonka, J., McAllister, D., Mackinnon, A., Joseph, J., Dwinell, M., Kalyanaraman, B., 2013. Mitochondria-targeted vitamin e analogs inhibit breast cancer cell energy metabolism and promote cell death. BMC Cancer 13, 285.

Cuéllar, A., Ramirez, J., Infante, V., Chavez, E., 1997. Further studies on the recoupling effect of 6-ketocholestanol upon oxidative phosphorylation in uncoupled liver mitochondria. FEBS Lett. 411, 365–368.

Cuezva, J., Krajewska, M., de Heredia, M., Krajewski, S., Santamaría, G., Kim, H., Zapata, J., Marusawa, H., Chamorro, M., Reed, J., 2002. The bioenergetic signature of cancer: a marker of tumor progression. Cancer Res. 62, 6674–6681.

de Pedro, N., Cautain, B., Melguizo, A., Vicente, F., Genilloud, O., Peláez, F., Tormo, J., 2013. Mitochondrial complex I inhibitors, acetogenins, induce HepG2 cell death through the induction of the complete apoptotic mitochondrial pathway. J. Bioenerg. Biomembr. 45, 153–164.

DeBerardinis, R., Mancuso, A., Daikhin, E., Nissim, I., Yudkoff, M., Wehrli, S., Thompson, C., 2007. Beyond aerobic glycolysis: transformed cells can engage in glutamine metabolism that exceeds the requirement for protein and nucleotide synthesis. Proc. Natl. Acad. Sci. U. S. A. 204, 19345–19350.

Diers, A., Vayalil, P., Oliva, C., Griguer, C., Darley-Usmar, V., Hurst, D., Welch, D., Landar, A., 2013. Mitochondrial bioenergetics of metastatic breast cancer cells in response to dynamic changes in oxygen tension: effects of HIF-1α. PLoS One 8, e68348.

Dobado, J.A., Gómez-Tamayo, J.C., Calvo-Flores, F.G., Martínez-García, H., Cardona, W., Weiss-López, B., Ramírez-Rodríguez, O., Pessoa-Mahana, H., Araya-Maturana, R., 2011. NMR assignment in regioisomeric hydroquinones. Magn. Reson. Chem. 49, 358–365.

Fantin, V., Berardi, M., Scorrano, L., Korsmeyer, S., Leder, P., 2002. A novel mitochondriotoxic small molecule that selectively inhibits tumor cell growth. Cancer Cell 2, 29–42.

Ferreira, J., 1990. Effect of butylated hydroxyanisole on electron transport in rat liver mitochondria. Biochem. Pharmacol. 40, 677–684.

Filomeni, G., Piccirillo, S., Graziani, I., Cardaci, S., Da Costa Ferreira, A., Rotilio, G., Ciriolo, M., 2009. The isatin-schiff base copper(II) complex Cu(isaepy)2 acts as delocalized lipophilic cation, yields widespread mitochondrial oxidative damage and induces AMP-activated protein kinase-dependent apoptosis. Carcinogenesis 30, 1115–1124.

Fones, E., Amigo, H., Gallegos, K., Guerrero, A., Ferreira, J., 1989. T-butyl-4-hydroxyanisole as an inhibitor of tumor cell respiration. Biochem. Pharmacol. 38, 3443–3451.

Galkin, A., Dröse, S., Brandt, U., 2006. The proton pumping stoichiometry of purified mitochondrial complex I reconstituted into proteoliposomes. Biochim. Biophys. Acta 1757, 1575–1581.

Gameiro, P., Laviolette, L., Kelleher, J., Iliopoulos, O., Stephanopoulos, G., 2013. Cofactor balance by nicotinamide nucleotide transhydrogenase (NNT) coordinates reductive carboxylation and glucose catabolism in the tricarboxylic acid (TCA) cycle. J. Biol. Chem. 288, 12967–12977.

Hail, N., Lotan, R., 2004. Apoptosis induction by the natural product cancer chemopreventive agent deguelin is mediated through the inhibition of mitochondrial bioenergetics. Apoptosis 9, 437–447.

Han, Y., Kim, S., Kim, S., Kim, S., Park, W., 2008. 2,4-dinitrophenol induces G1 phase arrest and apoptosis in human pulmonary adenocarcinoma calu-6 cells. Toxicol. in Vitro 22, 659–670.

Han, Y., Kim, S., Kim, S., Park, W., 2009. Carbonyl cyanide p-(trifluoromethoxy) phenylhydrazone (FCCP) as an O2(*-) generator induces apoptosis via the depletion of intracellular GSH contents in calu-6 cells. Lung Cancer 63, 201–209.

Hill, B., Benavides, G., Lancaster, J., Ballinger, S., Dell'Italia, L., Jianhua, Z., Darley-Usmar, V., 2012. Integration of cellular bioenergetics with mitochondrial quality control and autophagy. Biol. Chem. 393, 1485–1512.

Icard, P., Poulain, L., Lincet, H., 2012. Understanding the central role of citrate in the metabolism of cancer cells. Biochim. Biophys. Acta 1825, 111–116.

Jitschin, R., Hofmann, A., Bruns, H., Giessl, A., Bricks, J., Berger, J., Saul, D., Eckart, M., Mackensen, A., Mougiakakos, D., 2014. Mitochondrial metabolism contributes to oxidative stress and reveals therapeutic targets in chronic lymphocytic leukemia. Blood 123, 2663–2672.

Jose, C., Bellance, N., Rossignol, R., 2011. Choosing between glycolysis and oxidative phosphorylation: a tumor's dilemma? Biochim. Biophys. Acta 1807, 552–561.

Lou, P., Hansen, B., Olsen, P., Tullin, S., Murphy, M., Brand, M., 2007. Mitochondrial uncouplers with an extraordinary dynamic range. Biochem. J. 407, 129–140.

Martínez-Cifuentes, M., Weiss-López, B., Santos, L., Araya-Maturana, R., 2014. Intramolecular hydrogen bond in biologically active o-carbonyl hydroquinones. Molecules (Basel, Switz.) 19, 9354–9368.

Mendoza, L., Araya-Maturana, R., Cardona, W., Delgado-Castro, T., Garcia, C., Lagos, C., Cotoras, M., 2005. In Vitro sensitivity of botrytis cinerea to anthraquinone and anthrahydroquinone derivatives. J. Agric. Food Chem. 53, 10080–10084.

Mitchell, P., 1961. Coupling of phosphorylation to electron and hydrogen transfer by a chemi-osmotic type of mechanism. Nature 191, 144–148.

Miyoshi, H., 2001. Probing the ubiquinone reduction site in bovine mitochondrial complex I using a series of synthetic ubiquinones and inhibitors. J. Bioenerg. Biomembr. 33, 223–231.

Moreadith, R., Fiskum, G., 1984. Isolation of mitochondria from ascites tumor cells permeabilized with digitonin. Anal. Biochem. 137, 360–367.

Moreno-Sánchez, R., Marín-Hernández, A., Saavedra, E., Pardo, J.P., Ralph, S.J., Rodríguez-Enríquez, S., 2014. Who controls the ATP supply in cancer cells? Biochemistry lessons to understand cancer energy metabolism. Int. J. Biochem. Cell Biol. 50, 10–23.

Naven, R., Swiss, R., Klug-McLeod, J., Will, Y., Greene, N., 2013. The development of structure-activity relationships for mitochondrial dysfunction: uncoupling of oxidative phosphorylation. Toxicol. Sci. 131, 271–278.

Obre, E., Rossignol, R., 2015. Emerging concepts in bioenergetics and cancer research: metabolic flexibility, coupling, symbiosis, switch, oxidative tumors, metabolic remodeling, signaling and bioenergetic therapy. Int. J. Biochem. Cell Biol. 59, 167–181.

Okun, J., Lümmen, P., Brandt, U., 1999. Three classes of inhibitors share a common binding domain in mitochondrial complex I (NADH:ubiquinone oxidoreductase). J. Biol. Chem. 274, 2625–2630.

Panov, A., Orynbayeva, Z., 2013. Bioenergetic and antiapoptotic properties of mitochondria from cultured human prostate cancer cell lines PC-3, DU145 and LNCaP. PLoS One 8, e72078.

Pardo-Andreu, G., Nuñez-Figueredo, Y., Tudella, V., Cuesta-Rubio, O., Rodrigues, F., Pestana, C., Uyemura, S., Leopoldino, A., Alberici, L., Curti, C., 2011. The anti-cancer agent nemorosone is a new potent protonophoric mitochondrial uncoupler. Mitochondrion 11, 255–263.

Pedersen, P., Greenawalt, J., Reynafarje, B., Hullihen, J., Decker, G., Soper, J., Bustamente, E., 1978. Preparation and characterization of mitochondria and submitochondrial particles of rat liver and liver-derived tissues. Methods Cell Biol. 20, 411–484.

Pedroza, D., De Leon, F., Varela-Ramirez, A., Lema, C., Aguilera, R., Mito, S., 2014. The cytotoxic effect of 2-acylated-1,4-naphthohydroquinones on leukemia/lymphoma cells. Bioorg. Med. Chem. 22, 842–847.

Pereira, G.C., Branco, A.F., Matos, J.A., Pereira, S.L., Parke, D., Perkins, E.L., Serafim, T.L., Sardao, V.A., Santos, M.S., Moreno, A.J., Holy, J., Oliveira, P.J., 2007. Mitochondrially targeted effects of berberine [natural yellow 18, 5,6-dihydro-9,10-dimethoxybenzo(g)-1,3-benzodioxolo(5,6-a) quinolizinium] on K1735-M2 mouse melanoma cells: comparison with direct effects on isolated mitochondrial fractions. J. Pharmacol. Exp. Ther. 323, 636–649.

Plaza, C., Pavani, M., Faundez, M., Maya, J., Morello, A., Becker, M., De Ioannes, A., Cumsille, M., Ferreira, J., 2008. Inhibitory effect of nordihydroguaiaretic acid and its tetraacetylated derivative on respiration and growth of adenocarcinoma TA3 and its multiresistant variant TA3MTX-R. In Vivo 22, 353–361.

Rodríguez, J., Olea-Azar, C., Cavieres, C., Norambuena, E., Delgado-Castro, T., Soto-Delgado, J., Araya-Maturana, R., 2007. Antioxidant properties and free radical-scavenging reactivity of a family of hydroxynaphthalenones and dihydroxyanthracenones. Bioorg. Med. Chem. 15, 7058–7065.

Rodríguez-Enríquez, S., Torres-Márquez, M., Moreno-Sánchez, R., 2000. Substrate oxidation and ATP supply in AS-30D hepatoma cells. Arch. Biochem. Biophys. 375, 21–30.

Rydström, J., 2006. Mitochondrial NADPH, transhydrogenase and disease. Biochim. Biophys. Acta 1757, 721–726.

Satoh, T., Miyoshi, H., Sakamoto, K., Iwamura, H., 1996. Comparison of the inhibitory action of synthetic capsaicin analogues with various NADH-ubiquinone oxidoreductases. Biochim. Biophys. Acta 1273, 21–30.

Solaini, G., Sgarbi, G., Baracca, A., 2011. Oxidative phosphorylation in cancer cells. Biochim. Biophys. Acta 1807, 534–542.

Soto-Delgado, J., Bahamonde-Padilla, V., Araya-Maturana, R., Weiss-López, B., 2013. On the mechanism of biological activity of hydroquinone derivatives that inhibit tumor cell respiration. A theoretical study. Comput. Theor. Chem. 1013, 97–101.

Spycher, S., Smejtek, P., Netzeva, T., Escher, B., 2008. Toward a class-independent quantitative structure–activity relationship model for uncouplers of oxidative phosphorylation. Chem. Res. Toxicol. 21, 911–927.

Starkov, A., Dedukhova, V., Skulachev, V., 1994. 6-ketocholestanol abolishes the effect of the most potent uncouplers of oxidative phosphorylation in mitochondria. FEBS Lett. 355, 305–308.

Stein, L., Imai, S., 2012. The dynamic regulation of NAD metabolism in mitochondria. Trends Endocrinol. Metab. 23, 420–428.

Ueno, H., Miyoshi, H., Ebisui, K., Iwamura, H., 1994. Comparison of the inhibitory action of natural rotenone and its stereoisomers with various NADH-ubiquinone reductases. Eur. J. Biochem. 225, 411–417.

Urra, F.A., Martínez-Cifuentes, M., Pavani, M., Lapier, M., Jaña-Prado, F., Parra, E., Maya, J.D., Pessoa-Mahana, H., Ferreira, J., Araya-Maturana, R., 2013. An ortho-carbonyl substituted hydroquinone derivative is an anticancer agent that acts by inhibiting mitochondrial bioenergetics and by inducing G2/M-phase arrest in mammary adenocarcinoma TA3. Toxicol. Appl. Pharmacol. 267, 218–227.

Vega, A., Ramirez-Rodriguez, O., Martinez-Cifuentes, M., Ibanez, A., Araya-Maturana, R., 2009. 8,8-diethyl-1,4,5,8-tetrahydronaphthalene-1,4,5-trione. Acta Crystallogr. 65, o345.

Wang, Y., Perchellet, E.M., Ward, M.M., Lou, K., Hua, D.H., Perchellet, J.P., 2005. Rapid collapse of mitochondrial transmembrane potential in HL-60 cells and isolated mitochondria treated with anti-tumor 1,4-anthracenediones. Anti-Cancer Drugs 16, 853–867.

Wu, M., Neilson, A., Swift, A., Moran, R., Tamagnine, J., Parslow, D., Armistead, S., Lemire, K., Orrell, J., Teich, J., Chomicz, S., Ferrick, D., 2007. Multiparameter metabolic analysis reveals a close link between attenuated mitochondrial bioenergetic function and enhanced glycolysis dependency in human tumor cells. Am. J. Physiol. Cell. Physiol. 292, C125–C136.

Yizhak, K., Le Dévédec, S., Rogkoti, V., Baenke, F., de Boer, V., Frezza, C., Schulze, A., van de Water, B., Ruppin, E., 2014. A computational study of the Warburg effect identifies metabolic targets inhibiting cancer migration. Mol. Syst. Biol. 10, 744.

Zhang, X., Fryknäs, M., Hernlund, E., Fayad, W., De Milito, A., Olofsson, M., Gogvadze, V., Dang, L., Påhlman, S., Schughart, L., Rickardson, L., D'Arcy, P., Gullbo, J., Nygren, P., Larsson, R., Linder, S., 2014. Induction of mitochondrial dysfunction as a strategy for targeting tumour cells in metabolically compromised microenvironments. Nat. Commun. 5, 3295.

Zickermann, V., Wirth, C., Nasiri, H., Siegmund, K., Schwalbe, H., Hunte, C., Brandt, U., 2015. Structural biology. Mechanistic insight from the crystal structure of mitochondrial complex I. Science 347, 44–49.

Zu, X., Guppy, M., 2004. Cancer metabolism: facts, fantasy, and fiction. Biochem. Biophys. Res. Commun. 313, 459–465.